The Journal of Supercomputing (2025) 81:720
https://doi.org/10.1007/s11227-025-07181-2

Joint optimization for 6G beyond diagonal IRS-assisted multi-carrier NOMA vehicle-to-infrastructure communication

Manzoor Ahmed[1] · Wali Ullah Khan[2] · Mohammad Alamgeer[3] · Eatedal Alabdulkreem[4] · Shouki A. Ebad[5] · Ali M. Al-Sharafi[6] · Ashit Kumar Dutta[7] · Tahir Khurshaid[8]

Accepted: 13 March 2025
© The Author(s), under exclusive licence to Springer Science+Business Media, LLC, part of Springer Nature 2025

Abstract

The intelligent reconfigurable surface (IRS) is regarded as a highly promising technology for facilitating and enhancing the performance of future wireless communication networks. This is due to its capacity to effectively modify wireless channels in desired destinations with low-cost design and energy consumption. A significant amount of research has been dedicated to exploring the use of conventional IRS, where each phase response element is only connected to its own ground load with no connection to the other phase response elements. However, the simple design of conventional IRS limits its capacity to adjust passive beamforming. This study focuses on the implementation of beyond diagonal IRS (BD-IRS) in multi-carrier non-orthogonal multiple access (NOMA) vehicular communication, surpassing the use of diagonal phase shift matrices. Specifically, we propose a new optimization approach that aims to maximize the achievable spectral efficiency of a multi-carrier NOMA vehicular communication with BD-IRS assistance. This is achieved by optimizing the transmission power of RSU and the phase response of the BD-IRS. We utilize block coordinate descent and successive convex approximation methods to convert the original optimization problem into a series of subproblems. For the power allocation problem at RSU, we adopt Dinkelbach's and first-order Tayler approximation while exploiting unitary constraint transformation for the phase response problem at BD-IRS and then use the CVX toolbox for the solution. The numerical findings clearly illustrate the advantages of the proposed optimization framework and implementing BD-IRS in multi-carrier NOMA vehicular communications networks in comparison to the conventional IRS architecture.

Extended author information available on the last page of the article

Published online: 10 April 2025

Keywords Beyond diagonal intelligent reconfigurable surface · Non-orthogonal multiple access · Multi-carrier vehicular communication · Spectral efficiency optimization.

1 Introduction

The first five generations of wireless networks (1 G-5 G) have been effectively controlled by adjusting to the volatile wireless environment through the use of sophisticated designs at both the transmitting and receiving ends [1, 2]. In the context of future wireless networks, i.e., sixth-generation (6 G) and beyond, there is an expected utilization of an advanced technology known as intelligent reconfigurable surface (IRS) [3]. IRS enables the alteration of both the transceiver and the wireless environment, presenting promising progress in 6 G wireless networks [4]. The IRS system consists of multiple phase response elements that allow it to modify the wireless environment, resulting in enhanced spectrum and energy efficiency of the wireless network [5]. The efficiency of IRS technology has been substantiated in various wireless systems, including terrestrial and non-terrestrial networks [6]. IRS technology can operate in three modes, i.e., reflective mode, transmissive mode, and hybrid mode [7]. More specifically, IRS in reflective mode can offer half space overage and passively reflect an incident signal in the same direction. Thus, the transmitter and receiver must be located on the same side of the surface for efficient signal reflection [8]. Then, the transmissive IRS allows the incident signal to pass through the surface and reshape the phase shift of the signal toward the desired direction. In this mode, the IRS is located between the source and the destination nodes. Transmissive IRS is considered to be better than the reflective IRS because of self-interference in reflective IRS, as the source and destination are located on the same side of the surface. This can degrade the performance of the reflective IRS [9]. Furthermore, hybrid IRS has the feature of both reflective and transmissive IRS. In particular, hybrid IRS can simultaneously perform reflection and transmission for incident signals. This IRS is also called STAR IRS.

In addition to IRS, several air interface technologies such as non-orthogonal multiple access (NOMA), orthogonal time-frequency space, and rate splitting multiple access have emerged for efficient utilization of limited spectrum resources [10–12]. In particular, NOMA can improve spectral efficiency by multiplexing multiple users over the same spectrum simultaneously using different power levels based on the user's channel conditions [13]. More specifically, a transmitter can assign low power to a user with a strong channel condition and more power to a user with a weak channel condition. Then, the user with low transmit power and good channel condition can apply successive interference cancellation (SIC) to remove the signal of other users before decoding its own. In contrast, the one with more power and a weak channel can directly decode their signal by treating another user signal as noise.

Most of the present research is centered around using a conventional IRS model that has a diagonal phase shift matrix, commonly referred to as classical IRS [14,

15]. Each phase response element in this model is connected to its own adjustable impedance, without any connections to other phase response components on the surface [16]. More specifically, the conventional version of IRS is subject to two limitations. One limitation of the conventional IRS is its ability to solely modify the phase response of the input signal [15]. This constraint hampers its capacity to control passive beamforming, leading to a decline in performance. The second limitation is that it only allows signal reflection in the same direction, so limiting the coverage and capacity of the system. This implies that the transmitter and receiver must be positioned directly facing the traditional IRS system [17].

To address the limitations of conventional IRS and enhance the effectiveness of this developing technology, this study presents a novel approach called beyond diagonal IRS (BD-IRS) [18]. The updated version of the IRS family includes inter-phase response element connections, which despite increasing circuit complexity, greatly enhance system performance [19]. The mathematical model of BD-IRS is not limited to diagonal matrices. It encompasses a complete scattering phase response matrix, where various phase response elements are interconnected [20]. This study evaluates the achievable spectral efficiency performance of BD-IRS-assisted multi-carrier NOMA vehicular communication systems utilizing optimal power allocation at the roadside unit (RSU) and phase response design at BD-IRS.

Researchers have recently been incorporating BD-IRS into their proposed frameworks. The researchers in [21] have introduced a framework for optimizing transmit precoding and phase response design in multi-user wireless networks with the assistance of BD-IRS. The paper in [19] has presented a mathematical solution that enhances the average received signal and achievable rate of wireless networks with BD-IRS assistance. In [22], the authors have optimized the phase response of BD-IRS in both in order to maximize the received power of a multi-user system, considering both single antenna and multiple antennas at the transceiver. In addition, the study in [23] has introduced an optimization framework that takes into account mutual coupling in order to maximize the channel gain of the BD-IRS-assisted wireless system. In [24], the authors have introduced an optimization framework to examine various performance metrics in wireless systems assisted by BD-IRS. In addition, the study in [25] has examined the use of BD-IRS as a transmitter to evaluate the performance of wireless systems. Further, the authors of [26] have proposed a method to minimize power consumption in integrated sensing and communication systems using BD-IRS technology. Fang et al. [27] have conducted a study on the spectrum efficiency for multi-user wireless networks enabled by BD-IRS. Of late, the paper [28] has optimized power allocation and phase shift design in future transportation systems using orthogonal spectrum sharing.

Considering the existing advances in BD-IRS-assisted wireless networks, we note that the research on BD-IRS is in its early stages, with many open problems yet to be addressed. Based on this inspiration, we integrate the concept of BD-IRS in multi-carrier NOMA vehicular communication, which has not been previously explored in existing literature. This study is the inaugural research on multi-carrier NOMA vehicular communication with BD-IRS assistance, based on the available literature. Specifically, we want to enhance the achievable spectral efficiency of the

system by allocating optimal transmit power at RSU and phase response at BD-IRS while ensuring the minimum transmission rate of individual vehicle users (VUs). The primary contribution we have made can be succinctly expressed as follows.

- We consider a scenario of BD-IRS-assisted multi-carrier NOMA vehicular communication, wherein an RSU performs downlink transmission with J VUs using S carriers. To enhance the spectral efficiency of the system, we consider that RSU accommodates multiple VUs on each carrier. Hence, VUs on the same carrier receive NOMA interference after successive interference cancellation (SIC). Considering the urban area where maintaining the line of sight (LoS) links between RSU and VUs is challenging due to blockage. Resultantly, VUs can suffer from large-scale fading that can end up with poor system performance.
- To ensure smooth connectivity and improve the system performance, a BD-IRS system is mounted on an optimal location to assist communication between RSU and VUs. Thus, the signal from RSU can be received at UVs through both direct and indirect links. This work aims to enhance the achievable spectral efficiency of multi-carrier NOMA BD-IRS vehicular communication by optimizing the transmit power of RSU and phase response of BD-IRS. Due to the coupled variables and NOMA interference, the joint optimization is formulated as nonlinear programming and NP-hard problem.
- Achieving a joint optimization solution is complex computationally. We first make the optimization tractable by applying the block coordinate descent (BCD) and successive convex approximation (SCA) methods. Using these methods, the original optimization can be effectively transformed into a series of subproblems. Then, for the power allocation problem, we exploit Dinkelbach's and first-order Tayler approximation methods, while for the phase response problem at BD-IRS, we use unitary constraint for further transformation of both problems. In the end, we use the CVX toolbox for solving linear problems. Numerical results are carried out based on Monte Carlo simulations which demonstrate the effectiveness of BD-IRS compared to conventional IRS.

The rest of this work can be organized as follows. Section II discusses the proposed communication scenario and channel modeling, and formulates the spectral efficiency maximization problem. Section III illustrates the proposed solution to the formulated problem. Section IV provides and discusses the numerical results, comparison with benchmark conventional IRS framework, and their discussion.

2 System design, channel modeling, and problem formulation

In this section, we first study the considered scenario of BD-IRS-assisted multi-carrier vehicular communication, channel modeling between RSU and VUs, and various assumptions. Then, we formulate and discuss the spectral efficiency maximization problem.

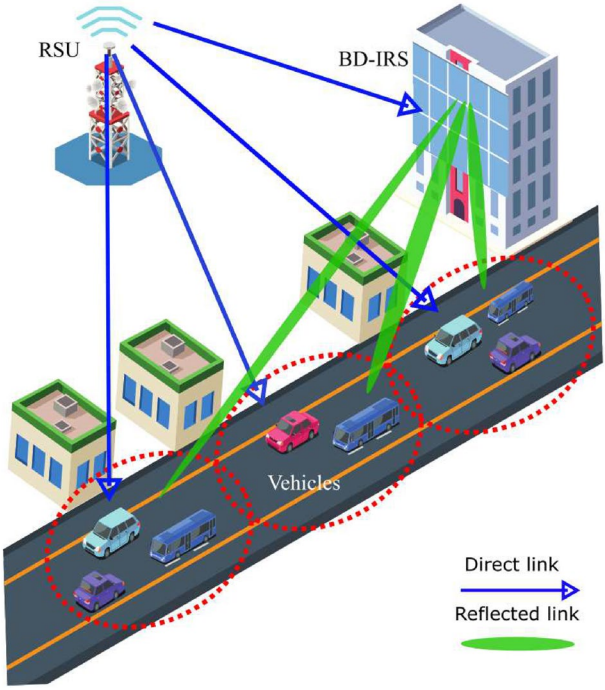

Fig. 1 BD-IRS-assisted multi-carrier NOMA vehicular network

2.1 System model and channel modeling

A downlink multi-carrier vehicular communication scenario is considered where RSU uses S carriers to communicate with J VUs using NOMA principle, as illustrated in Fig. 1. Let the set of S carriers can be defined as $\mathcal{S} = \{s|1, 2, 3, \ldots, S\}$, and the set of J VUs is denoted as $\mathcal{J} = \{j|1, 2, 3, \ldots, J\}$, respectively. The RSU and VUs are equipped with single antennas. We assume that RSU has complete information of all serving VUs [29]. Channel estimation is an important topic in advanced wireless networks and has been explored recently [30]. However, this work focuses on optimizing resources to maximize the system's energy efficiency, and estimating channels is beyond the scope of this work [31]. Considering the urban communication scenario, the VUs do not have always direct link from the RSU, hence experience large-scale fading due to signal blockage. A BD-IRS which operating in reflecting mode is considered to provide alternating link between VUs and RSU. Therefore, the VUs receive signals through direct and indirect links. The BD-IRS consists of I reflecting elements, the set of elements can be denoted as $\mathcal{I} = \{i|1, 2, 3, \ldots, I\}$. The superimposed signal of RSU for J VUs over s carrier can be stated as:

$$x_s = \sum_{j=1}^{J} \sqrt{p_{j,s}} x_{j,s}, \ \forall s, \tag{1}$$

where $p_{j,s}$ and $x_{j,s}$ are the transmit power and unit power signal of j VU over s carrier. The received signal of j VU over s carrier can be then expressed as:

$$y_{j,s} = \underbrace{(h_{j,s} + \mathbf{g}_{j,s}\boldsymbol{\phi}\mathbf{f}_{j,s})(p_{j,s} + \sum_{j'=j+1}^{J} p_{j',s})x_s}_{\text{superimposed signal}} + \underbrace{n_{j,s}}_{\text{AWGN}}, \ \forall s, \tag{2}$$

where $h_{j,s}$ is the channel gain of direct link between RSU and j VU over s carrier. The term $\mathbf{g}_{j,s} \in \mathbb{C}^{I\times 1}$ denotes the channel vector of j VU between RSU and BD-IRS over s carrier. $\boldsymbol{\phi} \in \mathbb{C}^{I\times I}$ shows the scattering matrix of BD-IRS which assume to satisfy $\boldsymbol{\phi}\boldsymbol{\phi}^H = \mathbf{I}_J$. $\mathbf{f}_{j,s} \in \mathbb{C}^{1\times I}$ denotes the channel vector of j VU from BD-IRS over s carrier. Moreover, $p_{j',s}$ is the interference power from other VUs after SIC decoding process while $n_{j,s}$ is the AWGN. The $\kappa_{j,s}$ channel can be modeled as $\kappa_{j,s} = \bar{\kappa}_{j,s} D_{j,s}^{-\beta/2}$, $\kappa \in \{h_{j,s}, \mathbf{g}_{j,s}, \mathbf{f}_{j,s}\}$, where $\kappa \sim \mathcal{CN}(0, \sigma^2)$ is the Rayleigh fading coefficient, D shows distance between two devices, and β is the path loss. For successful SIC process at the receiver side, the channel gains of j VUs over s carrier are assumed to be sorted as $h_{1,s} \leq h_{2,s} \leq \cdots \leq h_{j,s} \leq \cdots \leq h_{J,s}$. According to NOMA protocol, j VU applies SIC to subtract all other VUs signal with lower channel gains before decoding its own signal [32]. Then, it decodes signal with the other VUs with stronger channel gains by treating them noise. The signal-to-interference-plus-noise ratio (SINR) of j VU over s carrier based on the received signal can be expressed as:

$$\gamma_{j,s} = \frac{|h_{j,s} + \mathbf{G}|^2 p_{j,s}}{|h_{j,s} + \mathbf{G}|^2 \sum_{j'=j+1}^{J} p_{j',s} + \sigma^2}, \tag{3}$$

where $\mathbf{G} = \mathbf{g}_{j,s}\boldsymbol{\phi}\mathbf{f}_{j,s}$ and σ^2 is the variance of AWGN. Based on the SINR, the data rate of j VU over s carrier can be calculated as $R_{j,s} = \log_2(1 + \gamma_{j,s})$. The overall spectral efficiency of the vehicular communication considering the S carriers can be derived as:

$$R_{\text{sum}} = \sum_{s=1}^{S} \sum_{j=1}^{J} \log_2(1 + \gamma_{j,s}). \tag{4}$$

2.2 Problem formulation

The objective of this work is to maximize the spectral efficiency of the network, which can be achieved through joint optimization of RSU transmit power and

BD-IRS phase shift design.[1] The mathematical optimization for spectral efficiency maximization can be formulated as follows:

$$P_1 : \begin{cases} \max\limits_{(p_{j,s},\boldsymbol{\phi})} R_{\text{sum}} \\ C_1) : \sum\limits_{s=1}^{S}\sum\limits_{j=1}^{J} R_{j,s} \geq R_{\min}, \\ C_2) : \sum\limits_{s=1}^{S}\sum\limits_{j=1}^{J} p_{j,s} \leq P_{\max}, \\ C_3) : \boldsymbol{\phi}\boldsymbol{\phi}^H = \mathbf{I}_J, \end{cases} \tag{5}$$

where $R_{\min}$ denotes the minimum rate threshold requires for QoS of each VU and $P_{\max}$ the threshold for the maximum transmit power of RSU. The first constraint guarantees the QoS of each VU. The second constraint controls the transmit power of RSU, and the third constraint invokes for phase shift design of BD-IRS.

The optimization problem (5) is nonlinear due to the logarithmic function in the rate equation, and the fractional nature of the SINR $\gamma_{j,s}$ renders it non-convex. Additionally, the coupling of the decision variables, $p_{j,s}$ and $\boldsymbol{\phi}$, along with the unitary constraint C_3, classify it as NP-hard. Consequently, identifying the optimal solution is computationally intensive. To tackle this, we propose an iterative approach in the subsequent section by breaking down the joint optimization problem into manageable subproblems and addressing them iteratively.

3 Proposed solution

To address the joint optimization problem P_1 and enhance the spectral efficiency in the vehicular communication network, we propose a method that combines the BCD method and the SCA technique [33, 34]. This approach decouples the original problem into more manageable subproblems and iteratively solves them, converting the non-convex problem into a series of convex subproblems.

3.1 Transmit power allocation subproblem

Given the fixed value of $\boldsymbol{\phi}$, the sub-optimization problem for the transmit power allocation $p_{j,s}$ can be expressed as:

[1] The proposed optimization framework assumes that the carrier assignment to VUs has already been done before the optimization process. While the optimal carrier VUs assignment may further improve the system performance, it is beyond the scope of this work.

$$P_{1.1}: \begin{cases} \max\limits_{p_{j,s}} & \sum\limits_{s=1}^{S}\sum\limits_{j=1}^{J}\log_2\left(1+\gamma_{j,s}\right) \\ C_1): & \sum\limits_{s=1}^{S}\sum\limits_{j=1}^{J}R_{j,s}\geq R_{\min}, \\ C_2): & \sum\limits_{s=1}^{S}\sum\limits_{j=1}^{J}p_{j,s}\leq P_{\max}, \end{cases} \tag{6}$$

where $\gamma_{j,s}$ represents the SINR for the j-th VU on the s-th carrier, as referenced in (3). Additionally, the optimization problem described previously remains non-convex and nonlinear due to the logarithmic function in the objective function of (6). To tackle this issue and convert the non-convex problem into a convex format, we introduce a slack variable $t_{j,s}$ such that:

$$\log_2(1+\gamma_{j,s})\geq t_{j,s}. \tag{7}$$

Subsequently, we apply the inverse logarithmic transformation method to extract the SINR value from the logarithmic function, resulting in:

$$\gamma_{j,s}\geq 2^{t_{j,s}}-1. \tag{8}$$

Incorporating this slack variable, the sub-optimization problem becomes:

$$P_{1.2}: \begin{cases} \max\limits_{p_{j,s},t_{j,s}} & \sum\limits_{s=1}^{S}\sum\limits_{j=1}^{J}t_{j,s} \\ C_1): & \frac{|h_{j,s}+\mathbf{G}|^2 p_{j,s}}{|h_{j,s}+\mathbf{G}|^2\sum\limits_{j'=j+1}^{J}p_{j',s}+\sigma^2}\geq 2^{t_{j,s}}-1, \forall j,s, \\ C_2): & \sum\limits_{s=1}^{S}\sum\limits_{j=1}^{J}t_{j,s}\geq R_{\min}, \\ C_3): & \sum\limits_{s=1}^{S}\sum\limits_{j=1}^{J}p_{j,s}\leq P_{\max}. \end{cases} \tag{9}$$

Furthermore, the optimization problem (9) is presented in a more manageable form. However, incorporating the constraint C_1 from (9) remains a computationally demanding task. To tackle this issue, we employ Dinkelbach's method to convert the nonlinear term into a linear one. Define:

$$\alpha_{j,s}=|h_{j,s}+\mathbf{G}|^2,\quad \beta_{j,s}=\sum_{j'=j+1}^{J}p_{j',s}+\frac{\sigma^2}{|h_{j,s}+\mathbf{G}|^2}. \tag{10}$$

The SINR constraint becomes:

$$\frac{\alpha_{j,s}p_{j,s}}{\alpha_{j,s}\beta_{j,s}}\geq 2^{t_{j,s}}-1, \tag{11}$$

which simplifies to:

$$p_{j,s} \geq (2^{t_{j,s}} - 1)\beta_{j,s}. \tag{12}$$

Therefore, the problem can be reformulated as:

$$P_{1.3}: \begin{cases} \max\limits_{p_{j,s}, t_{j,s}} & \sum\limits_{s=1}^{S}\sum\limits_{j=1}^{J} t_{j,s} \\ C_1): & p_{j,s} \geq (2^{t_{j,s}} - 1)\beta_{j,s}, \forall j, s, \\ C_2): & \sum\limits_{s=1}^{S}\sum\limits_{j=1}^{J} R_{j,s} \geq R_{\min}, \\ C_3): & \sum\limits_{s=1}^{S}\sum\limits_{j=1}^{J} p_{j,s} \leq P_{\max}. \end{cases} \tag{13}$$

Then By applying the first-order Taylor approximation, we linearize the exponential term around $t_{j,s}^{(t)}$:

$$2^{t_{j,s}} \approx 2^{t_{j,s}^{(t)}} \ln(2)(t_{j,s} - t_{j,s}^{(t)}) + 2^{t_{j,s}^{(t)}}. \tag{14}$$

Substituting back, we get:

$$p_{j,s} \geq \left[2^{t_{j,s}^{(t)}} \ln(2)(t_{j,s} - t_{j,s}^{(t)}) + 2^{t_{j,s}^{(t)}} - 1\right]\beta_{j,s}. \tag{15}$$

This approximation ensures that the problem is now convex. Thus, the reformulated problem becomes:

$$P_{1.4}: \begin{cases} \max\limits_{p_{j,s}, t_{j,s}} & \sum\limits_{s=1}^{S}\sum\limits_{j=1}^{J} t_{j,s} \\ C_1): & p_{j,s} \geq \left[2^{t_{j,s}^{(t)}} \ln(2)(t_{j,s} - t_{j,s}^{(t)}) + 2^{t_{j,s}^{(t)}} - 1\right]\beta_{j,s}, \ \forall j, s, \\ C_2): & \sum\limits_{s=1}^{S}\sum\limits_{j=1}^{J} t_{j,s} \geq R_{\min}, \\ C_3): & \sum\limits_{s=1}^{S}\sum\limits_{j=1}^{J} p_{j,s} \leq P_{\max}. \end{cases} \tag{16}$$

Following this, the optimization problem (identified as equation 16) is reformulated into a simpler and convex structure, facilitating effective solution through convex optimization tools like CVX [35]. Additionally, the demonstration of convexity is detailed in Sect. 3.1.1. Furthermore, a comprehensive explanation and operational methodology are illustrated in Algorithm 1.

3.1.1 Proof of convexity

We need to show that the transformed problem is convex. By introducing the slack variable $t_{j,s}$ and linearizing the exponential term, we ensure that the objective function $\sum_{s=1}^{S}\sum_{j=1}^{J} t_{j,s}$ is linear. The constraints are also linearized, maintaining the convexity

of the feasible region. The constraint $p_{j,s} \geq \left[2^{t_{j,s}^{(t)}} \ln(2)(t_{j,s} - t_{j,s}^{(t)}) + 2^{t_{j,s}^{(t)}} - 1\right]\beta_{j,s}$ ensures that the feasible region is convex, as the linear approximation retains the convexity within the feasible region. Therefore, the overall problem is convex.

Algorithm 1 BCD-SCA for Power Allocation

Initialization:
Initialize transmit power $p_{j,s}$ for all VUs j and carriers s
Set iteration index $t = 0$
Choose convergence tolerance ϵ
Compute initial SINR values $\gamma_{j,s}$
Compute initial slack variables $t_{j,s} = \log_2(1 + \gamma_{j,s})$
repeat
  Step 1: Update SINR values
  For each VU j and carrier s, update $\gamma_{j,s}$
  Step 2: Update slack variables
  For each VU j and carrier s, set $t_{j,s} = \log_2(1 + \gamma_{j,s})$
  Step 3: Linearize the SINR constraint
  Apply first-order Taylor expansion to $2^{t_{j,s}}$
  Step 4: Solve the convex optimization problem
  Solve the convex problem (16).
  Step 5: Update power allocation
  Set $p_{j,s}$ to the solution obtained from the convex optimization problem
  Step 6: Check for convergence
  Compute the difference $\Delta p_{j,s}$
  If $\Delta p_{j,s} < \epsilon$, set convergence flag to true
  Increment iteration index $t = t + 1$
until convergence flag is true
Output: Optimized transmit power allocation $p_{j,s}$

3.1.2 Complexity and convergence analysis

3.1.2.1 Complexity analysis The proposed BCD-SCA algorithm involves iteratively solving a series of convex optimization problems. The primary computational steps include:

1. *Initialization*: Initializing the transmit power allocation $p_{j,s}$ and computing initial SINR values $\gamma_{j,s}$. This step has a complexity of $\mathcal{O}(JS)$ where J is the number of VUs and S is the number of carriers.
2. *SINR Update*: Updating the SINR values $\gamma_{j,s}$ in each iteration, which involves calculating the ratio of powers and has a complexity of $\mathcal{O}(JS)$.
3. *Slack Variable Update*: Computing the slack variables $t_{j,s}$, which also has a complexity of $\mathcal{O}(JS)$.
4. *Convex Optimization*: Solving the convex optimization problem. Given the problem size, this step typically involves an interior-point method or similar, with complexity approximately $\mathcal{O}((JS)^{3/2})$.

In general, the complexity per iteration is dominated by the convex optimization step, leading to an iteration complexity of $\mathcal{O}((JS)^{3/2})$. The total complexity depends on the number of iterations T, resulting in a total complexity of $\mathcal{O}(T(JS)^{3/2})$.

3.1.2.2 Convergence analysis The convergence of the BCD-SCA algorithm can be analyzed by considering the following aspects:

1. *Convex Approximation*: Each iteration involves solving a convex optimization problem, which guarantees finding a local optimum for the subproblem. Since convex problems have well-defined global optima, each iteration provides an optimal update for the given linearization.
2. *Monotonic Improvement*: The iterative process ensures that the objective function, the sum of the slack variables $\sum t_{j,s}$, is non-decreasing. This is because each step maximizes the objective under the current constraints.
3. *Convergence Criteria*: The algorithm terminates when the difference between consecutive power allocations, $\Delta p_{j,s}$, falls below a predefined threshold ϵ. This ensures that the solution stabilizes and does not change significantly with further iterations.

Given the properties of convex optimization and the monotonic improvement of the objective function, the BCD-SCA algorithm is guaranteed to converge to a stationary point. The choice of the convergence tolerance ϵ determines the precision of the solution and the number of iterations required. In practice, selecting an appropriate ϵ balances convergence speed and solution precision.

3.2 Phase shift optimization problem

Given the fixed value for the transmission power control, the sub-optimization problem for the phase shift control can be expressed as:

$$P_{2.1}: \begin{cases} \max\limits_{\boldsymbol{\phi}} \quad R_{\text{sum}} \\ C_1): \sum\limits_{s=1}^{S}\sum\limits_{j=1}^{J} R_{j,s} \geq R_{\min}, \\ C_2): \boldsymbol{\phi}\boldsymbol{\phi}^H = \mathbf{I}_I. \end{cases} \tag{17}$$

In the above-mentioned optimization problem, the unitary constraint C_2 for the IRS phase shifts needs to be transformed into a more relaxed form. The motivation for the convexity of the objective function with respect to $\boldsymbol{\phi}$ arises from the fact that $\boldsymbol{\phi}$ reflects the signal toward the users uniformly.

3.2.1 Unitary constraint transformation

To handle the unitary constraint $\boldsymbol{\phi}\boldsymbol{\phi}^H = \mathbf{I}_I$, we consider a relaxed constraint that ensures each element of $\boldsymbol{\phi}$ lies on the unit circle. Specifically, we represent $\boldsymbol{\phi}$ as $\boldsymbol{\phi} = \text{diag}(\mathbf{v})$ where $\mathbf{v} \in \mathbb{C}^I$ and $|v_i| = 1$ for all i. This transformation allows us to rewrite the unitary constraint in a more tractable form.

The relaxed constraint is given by:

$$|v_i|^2 = v_i v_i^H = 1, \quad \forall i. \tag{18}$$

To understand why this transformation is valid, consider that the original constraint $\boldsymbol{\phi}\boldsymbol{\phi}^H = \mathbf{I}_I$ ensures that $\boldsymbol{\phi}$ is a unitary matrix, meaning all its columns are orthonormal. By relaxing this to a diagonal matrix with unit-modulus elements, we preserve the essential property that each phase shift element affects the magnitude of the signal uniformly, which is crucial for beamforming. This constraint can be incorporated into the optimization problem as follows:

$$P_{2.2} : \begin{cases} \max\limits_{\mathbf{v}} \quad R_{\text{sum}} \\ C_1) : \sum\limits_{s=1}^{S} \sum\limits_{j=1}^{J} R_{j,s} \geq R_{\min}, \\ C_2) : |v_i|^2 = 1, \quad \forall i. \end{cases} \tag{19}$$

By introducing the vector $\mathbf{v}$, we can reframe the problem in terms of optimizing the phase shifts directly, which simplifies the mathematical manipulation. The constraint $|v_i| = 1$ implies that each element of $\mathbf{v}$ must lie on the complex unit circle, i.e., each element has a magnitude of 1. This condition can be expressed as:

$$v_i = e^{j\theta_i}, \quad \forall i, \tag{20}$$

where θ_i is the phase angle of the i-th element. This parameterization ensures that the phase shifts are bounded in the complex plane, maintaining the unit-modulus property essential for effective IRS beamforming.

Next, we incorporate this relaxed unitary constraint into the SINR expression. Given the original SINR for user j and carrier s:

$$\gamma_{j,s} = \frac{|h_{j,s} + \mathbf{g}_{j,s}\text{diag}(\mathbf{v})\mathbf{f}_{j,s}|^2 p_{j,s}}{|h_{j,s} + \mathbf{g}_{j,s}\text{diag}(\mathbf{v})\mathbf{f}_{j,s}|^2 \sum\limits_{j'=j+1}^{J} p_{j',s} + \sigma^2}. \tag{21}$$

The term $\mathbf{g}_{j,s}\text{diag}(\mathbf{v})\mathbf{f}_{j,s}$ can be simplified by defining:

$$\mathbf{G}_{j,s} = \mathbf{g}_{j,s} \odot \mathbf{f}_{j,s}, \tag{22}$$

where $\odot$ denotes the Hadamard (element-wise) product. Thus, the SINR becomes:

$$\gamma_{j,s} = \frac{|h_{j,s} + \mathbf{G}_{j,s}\mathbf{v}|^2 p_{j,s}}{|h_{j,s} + \mathbf{G}_{j,s}\mathbf{v}|^2 \sum_{j'=j+1}^{J} p_{j',s} + \sigma^2}. \tag{23}$$

This reformulation allows us to directly optimize over the phase shift vector $\mathbf{v}$ while respecting the unit-modulus constraint. This makes the problem more tractable and enables the use of efficient optimization techniques to solve the phase shift design problem under the relaxed unitary constraint. Moreover by following the convex approximation transformation done in Sect. 3.1, the convex sub-optimization problem can be expressed as follows:

$$P_{2.3}: \begin{cases} \max\limits_{\mathbf{v}, t_{j,s}} & \sum\limits_{s=1}^{S}\sum\limits_{j=1}^{J} t_{j,s} \\ C_1): & \alpha_{j,s} p_{j,s} \geq \Gamma, \quad \forall j, s, \\ C_2): & |v_i|^2 = 1, \quad \forall i, \\ C_3): & \sum\limits_{s=1}^{S}\sum\limits_{j=1}^{J} R_{j,s} \geq R_{\min}, \end{cases} \tag{24}$$

where $\Gamma = \left[2^{t_{j,s}^{(t)}} \ln(2)(t_{j,s} - t_{j,s}^{(t)}) + 2^{t_{j,s}^{(t)}} - 1\right]\beta_{j,s}$. This method makes the problem convex, simplifying the optimization of phase shifts by relaxing the unitary constraint with the help of convex optimization tools like CVX. Additionally, a detailed explanation and the operational principles are depicted in Algorithm 2.

3.2.2 Complexity and convergence analysis

3.2.2.1 Complexity analysis The proposed BCD-SCA algorithm for phase shift optimization involves iteratively solving a series of convex optimization problems. The primary computational steps include:

1. *Initialization*: Initializing the phase shift matrix $\boldsymbol{\phi}$ and computing initial SINR values $\gamma_{j,s}$. This step has a complexity of $\mathcal{O}(IS)$ where I is the number of reflecting elements and S is the number of carriers.
2. *SINR Update*: Updating the SINR values $\gamma_{j,s}$ in each iteration, which involves calculating the ratio of powers and has a complexity of $\mathcal{O}(JS)$.
3. *Slack Variable Update*: Computing the slack variables $t_{j,s}$, which also has a complexity of $\mathcal{O}(JS)$.
4. *Convex Optimization*: Solving the convex optimization problem. Given the problem size, this step typically involves an interior-point method or similar, with complexity approximately $\mathcal{O}((IS)^{3/2})$.

Overall, the complexity per iteration is dominated by the convex optimization step, leading to an iteration complexity of $\mathcal{O}((IS)^{3/2})$. The total complexity depends on the number of iterations T, resulting in a total complexity of $\mathcal{O}(T(IS)^{3/2})$.

Table 1 Simulation parameters

Parameter	Symbol	Value
Number of vehicle users (VUs)	J	10
Number of carriers	S	4
Number of reflecting elements	I	50
Minimum required rate	$R_{\min}$	2 Mbps
Maximum transmit power of RSU	$P_{\max}$	40 dBm
Noise power spectral density	σ^2	−174 dBm/Hz
Path loss exponent	β	3
Distance between RSU and VUs	$D_{j,s}$	100 m (variable)
Initial phase shift values	$\mathbf{v}^{(0)}$	Random with $\lvert v_i \rvert = 1$
Convergence tolerance	ϵ	10^{-3}
Iteration limit	T	1000
Carrier frequency	f_c	2.4 GHz
Bandwidth per carrier	B	10 MHz

3.2.2.2 Convergence analysis The convergence of the BCD-SCA algorithm can be analyzed by considering the following aspects:

1. *Convex Approximation*: Each iteration involves solving a convex optimization problem, which guarantees finding a local optimum for the subproblem. Since convex problems have well-defined global optima, each iteration provides an optimal update for the given linearization.
2. *Monotonic Improvement*: The iterative process ensures that the objective function, the sum of the slack variables $\sum t_{j,s}$, is non-decreasing. This is because each step maximizes the objective under the current constraints.
3. *Convergence Criteria*: The algorithm terminates when the difference between consecutive updates of $\boldsymbol{\phi}$, falls below a predefined threshold ϵ. This ensures that the solution stabilizes and does not change significantly with further iterations.

Given the properties of convex optimization and the monotonic improvement of the objective function, the BCD-SCA algorithm is guaranteed to converge to a stationary point. The choice of the convergence tolerance ϵ determines the accuracy of the solution and the number of iterations required. In practice, selecting an appropriate ϵ balances convergence speed and solution precision.

Algorithm 2 BCD-SCA for Phase Shifts

Initialization:
Initialize phase shift vector $\mathbf{v}$ such that $|v_i| = 1$ for all i
Set iteration index $t = 0$
Choose convergence tolerance ϵ
Compute initial SINR values $\gamma_{j,s}$
Compute initial slack variables $t_{j,s} = \log_2(1 + \gamma_{j,s})$
repeat
  Step 1: Update SINR values
  For each VU j and carrier s, calculate: (23)
  Step 2: Update slack variables
  For each VU j and carrier s, set:

$$t_{j,s}^{(t)} = \log_2(1 + \gamma_{j,s}^{(t)})$$

  Step 3: Solve the convex optimization problem
  Solve the following convex problem (24) using a CVX:
  Step 4: Update phase shift vector
  Set $\mathbf{v}^{(t+1)}$ to the solution obtained from the convex optimization problem
  Step 5: Check for convergence
  Compute the difference between consecutive phase shift vectors:

$$\Delta \mathbf{v} = \|\mathbf{v}^{(t+1)} - \mathbf{v}^{(t)}\|$$

  If $\Delta \mathbf{v} < \epsilon$, set convergence flag to true
  Increment iteration index $t = t + 1$
until convergence flag is true
Output: Optimized phase shift vector $\mathbf{v}$

4 Results and discussion

This section details the numerical outcomes that validate the effectiveness of the proposed method. Detailed simulations were performed based on the parameters described in Table 1. To further validate the effectiveness of the proposed method, its performance was compared with several recognized benchmarks including: Conventional IRS (Conv. IRS) [36], Random Phase, Random Power, and Orthogonal Multiple Access (OMA) [37]. Subsequently, comprehensive simulations were conducted on independent channel realizations and the average outcomes were produced. Furthermore, the effectiveness of the proposed scheme was also evaluated against the interior-point method (Int. Point) [38] to further confirm the validity of the findings.

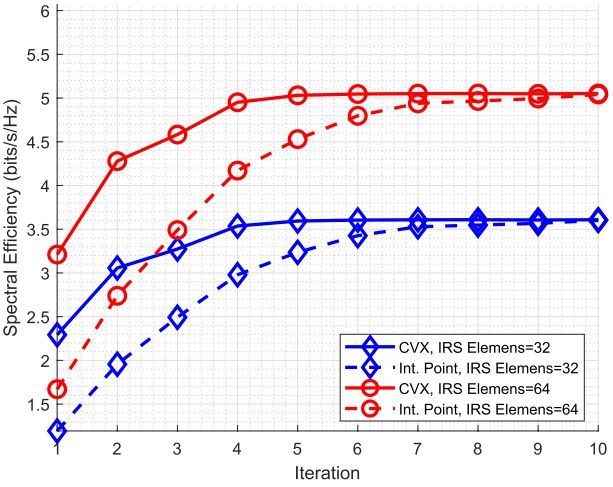

Fig. 2 Convergence analysis: number of iterations versus spectral efficiency for different RIS elements

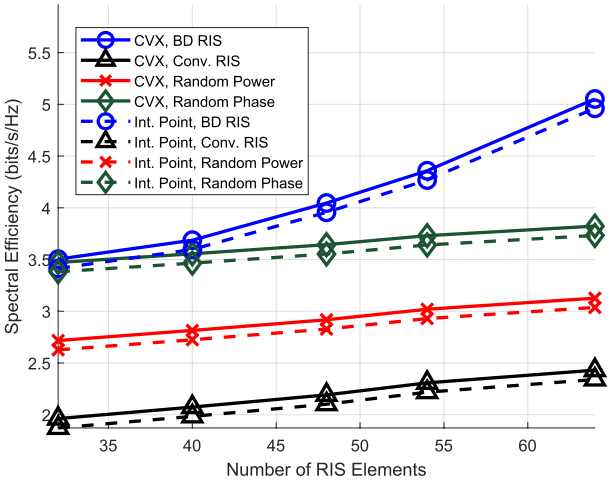

Fig. 3 Impact of IRS size on system performance: number of phase shift elements in RIS versus spectral efficiency of the proposed framework and benchmark frameworks

4.1 Discussion

Prior to delving into the specifics and assessing the efficacy of the proposed scheme (BD-IRS with NOMA), it is crucial to examine the convergence of the algorithm. To achieve this, simulations were conducted by adjusting the number of IRS elements $I = [32, 64]$ utilizing both the CVX and Int. Point methods. Results shown in Fig. 2 indicate that the algorithm stabilizes after several iterations. Additionally, it has been observed that the time required for convergence varies with different

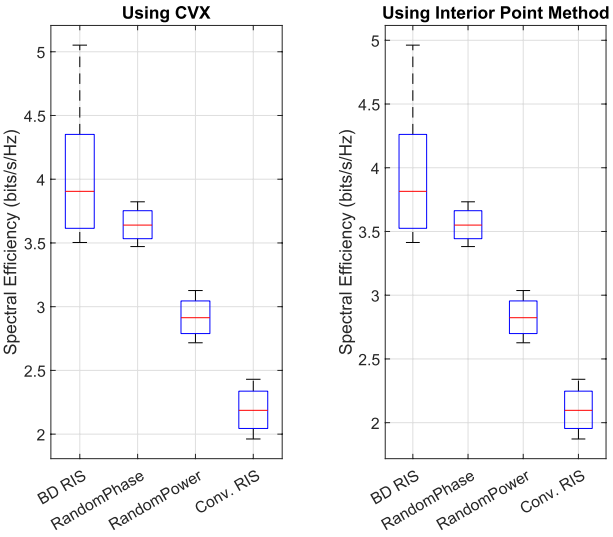

Fig. 4 Statistical review of CVX versus interior-point methods for different optimization frameworks

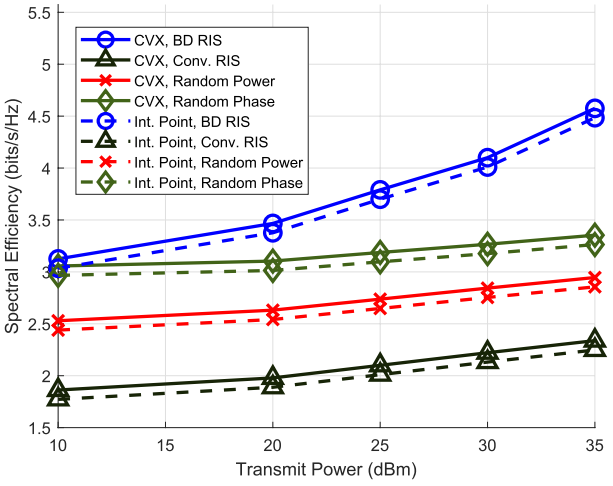

Fig. 5 Effect of transmission power on system performance: varying available power at RSU versus spectral efficiency for the proposed framework and benchmark frameworks

simulation parameters. This variation stems from the fact that increasing simulation parameters in the system necessitates more time to determine the optimal solution.

Furthermore, following the demonstration of the proposed scheme's effectiveness, simulations were conducted with $J = 10$, $P_{\max} = 20$ dBm, and varying IRS elements $I = [32, 64]$. The simulations also utilized both the CVX and Interior Point methods in various benchmark schemes, including random power and phase, as well as the conventional IRS. The results shown in Fig. 3 indicate that as the number of

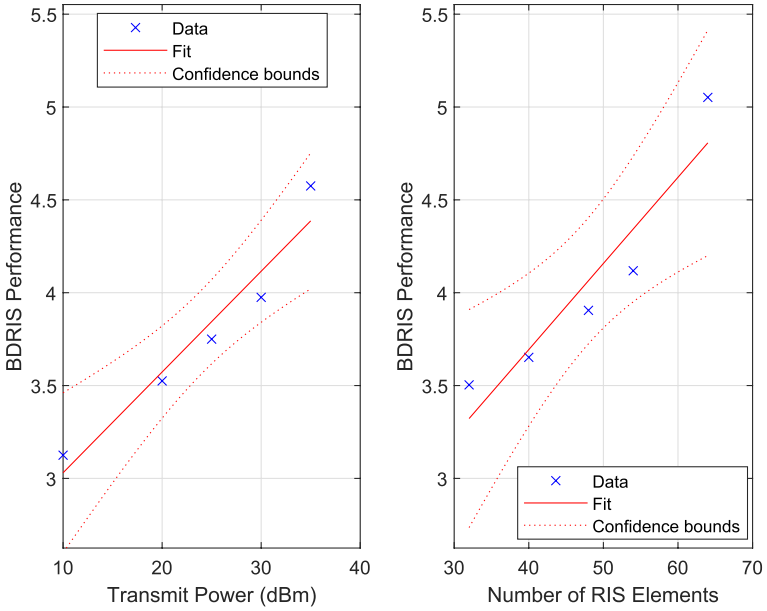

Fig. 6 Regression analysis for both varying transmit power and RIS elements

IRS elements increases, the system performance improves. It was also discovered that for a smaller number of IRS elements, the performance of both the random and optimal phases for BD-IRS is identical. However, as the number of IRS elements increases, the BD-IRS begins to outperform the others.

Furthermore, the entire simulation was conducted using both the CVX and Interior Point methods. The statistical analysis presented in Fig. 4 demonstrates the performance of each method across different metrics. In the case of BD-IRS, CVX marginally surpasses Interior Point (mean: 4.0461 vs. 3.9561). This pattern is consistent for the Random Phase and Random Power metrics as well. *T*-tests indicate no significant differences in the means for BD-IRS ($p = 0.8213$), implying that the two methods are effectively equivalent. While CVX tends to perform slightly better, Interior Point also provides competitive results.

Subsequently, to further reveal the effectiveness of the proposed scheme, extensive simulations were conducted across various levels of transmit power. The results in Fig. 5 demonstrate that the proposed scheme continues to outperform others, even at lower levels of transmit power. Furthermore, as the transmit power increases, it begins to perform better than the alternatives.

Furthermore, to explore the effects of IRS elements in comparison to the transmit power levels on system performance, a regression analysis is presented in Fig. 6. This analysis reveals a strong positive correlation between both transmit power and the number of IRS elements on BD-IRS performance. Specifically, the transmit power model indicates an intercept of 2.4878 and a slope of 0.0543, with a high *R*-squared value of 0.935, implying that 93.5% of the variability in BD-IRS performance can be attributed to transmit power. Regarding the number of IRS elements,

Table 2 Regression analysis results

Parameter	Transmit power	Number of IRS elements
Intercept	2.4878 ($p = 0.0013$)	1.8377 ($p = 0.0300$)
Slope	0.0543 ($p = 0.0071$)	0.0464 ($p = 0.0171$)
R-squared	0.935	0.885
Adjusted R-squared	0.914	0.847

the model estimates an intercept of 1.8377 and a slope of 0.0464, with an R-squared value of 0.885, suggesting that 88.5% of the variability is accounted for by the number of IRS elements. Both factors show statistically significant coefficients (p-values< 0.05), underscoring their substantial impact. Although both factors are highly significant, the slightly higher R-squared value for transmit power indicates a somewhat greater effect on BD-IRS performance. Additionally, the regression analysis is detailed in Table 2

Furthermore, to showcase the efficacy of the proposed approach, simulations were carried out using BD-IRS and Conventional IRS, integrating both NOMA and OMA techniques. These simulations employed CVX and interior-point methods as well. The findings depicted in Fig. 7 indicate that with constant transmit power levels, system performance initially increases with rising SINR values. Yet, at a SINR of about 20 dBm, a peak is reached after which performance starts to deteriorate. Despite these conditions, the BD-IRS with NOMA configuration still surpasses the alternative setups, underscoring the success of our method. Additionally, on average, BD-IRS with NOMA shows a performance enhancement of roughly 24.91% over TD-IRS with NOMA and 42.71% over Conv. IRS with OMA for the range of SINR values.

5 Conclusions

Due to advanced beamforming capability, BD-IRS is considered to be one of the potential technologies for 6 G wireless networks to extend wireless coverage, enhance capacity, and support massive connectivity. This study presented a new vehicular communication scenario that utilizes the BD-IRS with multi-carrier downlink NOMA. In particular, our work proposed an optimization framework to maximize the achievable spectral efficiency of BD-IRS-assisted multi-carrier NOMA vehicular communication systems. The optimization approach we proposed simultaneously optimizes the power allocation of RSU and the phase response of BD-IRS, considering various practical constraints. Because the specified joint problem was a combination of nonlinear and NP-hard, we utilized the BCD and SCA approaches to divide the optimization into a series of subproblems. Subsequently, each problem undergoes a conversion into a linear problem prior to the application of a conventional convex optimization technique for an optimal solution. Numerical results demonstrate that BD-IRS-assisted multi-carrier NOMA

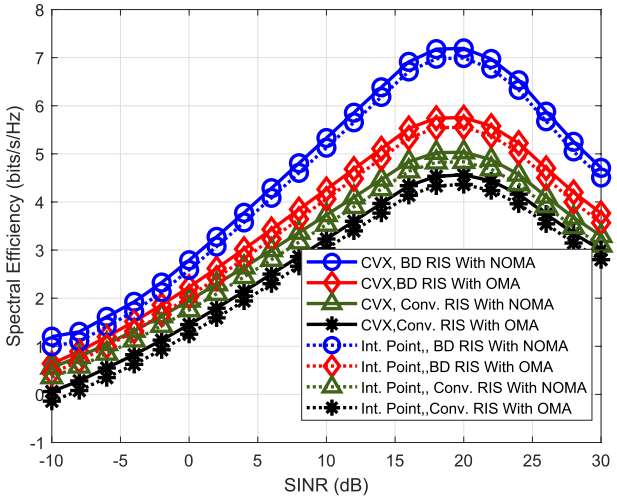

Fig. 7 Effect of received signal strength on system performance: varying SINR values versus spectral efficiency for the proposed optimization and benchmark schemes

vehicular communication outperforms the benchmark conventional IRS-assisted vehicular communication system. Future investigations can consider NOMA and BD-RIS in multi-carrier non-terrestrial communication scenarios. This will result in more complex and challenging problems due to the high path loss and Dopler effect in non-terrestrial systems.

Acknowledgements This work was supported in part by the Deanship of Research and Graduate Studies at King Khalid University for funding this work through Large Research Project under Grant RGP2/158/45; in part by the Researchers Supporting Project through Princess Nourah bint Abdulrahman University, Riyadh Saudi Arabia, under Grant PNURSP2025R114; in part by the Deanship of Scientific Research at Northern Border University, Arar, Saudi Arabia, under Grant NBU-FFR-2025-1564; in part by the Department of Computer Science and Artificial Intelligence, College of Computing and Information Technology, University of Bisha, Bisha, Saudi Arabia; in part by the Researchers Supporting Project through Almaarefa University, Riyadh, Saudi Arabia, under Grant MHIRSP2024005.

Author Contributions M.A. and W.U.K. wrote the main manuscript text. M.A., E.A., S.E., A.A., A.D., and A.S. read and review the paper.

Data availability No datasets were generated or analyzed during the current study.

Declarations

Conflict of interest The authors declare no competing interests.

References

1. Vaezi M, Azari A, Khosravirad SR, Shirvanimoghaddam M, Azari MM, Chasaki D, Popovski P (2022) Cellular, wide-area, and non-terrestrial iot: a survey on 5g advances and the road toward 6g. IEEE Commun Surv Tutor 24(2):1117–1174. https://doi.org/10.1109/COMST.2022.3151028

2. Wang H, Guo P, Li X, Wen F, Wang X, Nallanathan A (2024) Mbpd: a robust algorithm for polar-domain channel estimation in near-field wideband xl-mimo systems. IEEE Internet Things J. https://doi.org/10.1109/JIOT.2024.3477573
3. Khan WU, Lagunas E, Ali Z, Javed MA, Ahmed M, Chatzinotas S, Ottersten B, Popovski P (2022) Opportunities for physical layer security in uav communication enhanced with intelligent reflective surfaces. IEEE Wirel Commun 29(6):22–28. https://doi.org/10.1109/MWC.001.2200125
4. Deng M et al (2024) Reconfigurable intelligent surfaces enabled vehicular communications: a comprehensive survey of recent advances and future challenges. IEEE Trans Intell Vehic. https://doi.org/10.1109/TIV.2024.3476934
5. Ahmed M, Soofi AA et al (2025) Advancements in ris-assisted uav for empowering multi-access edge computing: a survey. IEEE Internet Things J. https://doi.org/10.1109/JIOT.2025.3527041
6. Ahmed M, Wahid A, Laique SS, Khan WU, Ihsan A, Xu F, Chatzinotas S, Han Z (2023) A survey on star-ris: use cases, recent advances, and future research challenges. IEEE Internet Things J 10(16):14689–14711. https://doi.org/10.1109/JIOT.2023.3279357
7. Khan WU, Mahmood A, Jamshed MA, Lagunas E, Ahmed M, Chatzinotas S (2025) Beyond diagonal ris for 6g non-terrestrial networks: potentials and challenges. IEEE Netw 39(1):80–89. https://doi.org/10.1109/MNET.2024.3480332
8. Ahmed M, Raza S, Soofi AA, Khan F, Khan WU, Xu F, Chatzinotas S, Dobre OA, Han Z (2024) A survey on reconfigurable intelligent surfaces assisted multi-access edge computing networks: state of the art and future challenges. Comput Sci Rev 54:100668
9. Ahmed M, Raza S, Soofi AA, Khan F, Khan WU, Abideen SZU, Xu F, Han Z (2024) Active reconfigurable intelligent surfaces: expanding the frontiers of wireless communication-a survey. IEEE Commun Surv Tutor. https://doi.org/10.1109/COMST.2024.3423460
10. Khan WU, Jameel F, Ristaniemi T, Khan S, Sidhu G, Liu J (2020) Joint spectral and energy efficiency optimization for downlink noma networks. IEEE Trans Cognit Commun Netw 6(2):645–656. https://doi.org/10.1109/TCCN.2019.2945802
11. Wang H, Chen Q, Wang X, Du W, Li X, Nallanathan A (2025) Adaptive block sparse backtracking-based channel estimation for massive mimo-otfs systems. IEEE Internet Things J 12(1):673–682. https://doi.org/10.1109/JIOT.2024.3466911
12. Khan WU, Ali Z, Lagunas E, Mahmood A, Asif M, Ihsan A, Chatzinotas S, Ottersten B, Dobre OA (2023) Rate splitting multiple access for next generation cognitive radio enabled leo satellite networks. IEEE Trans Wireless Commun 22(11):8423–8435. https://doi.org/10.1109/TWC.2023.3263116
13. Ahmed A, Xingfu W, Hawbani A, Yuan W, Tabassum H, Liu Y, Qaisar MUF, Ding Z, Al-Dhahir N, Nallanathan A, Ng DWK (2024) Unveiling the potential of noma: a journey to next generation multiple access. IEEE Commun Surv Tutor. https://doi.org/10.1109/COMST.2024.3521647
14. Liu Y, Liu X, Mu X, Hou T, Xu J, Di Renzo M, Al-Dhahir N (2021) Reconfigurable intelligent surfaces: principles and opportunities. IEEE Commun Surv Tutor 23(3):1546–1577. https://doi.org/10.1109/COMST.2021.3077737
15. Khan WU, Lagunas E, Mahmood A, Ali Z, Asif M, Chatzinotas S, Ottersten B (2023) Integration of noma with reflecting intelligent surfaces: a multi-cell optimization with sic decoding errors. IEEE Trans Green Commun Netw 7(3):1554–1565. https://doi.org/10.1109/TGCN.2023.3263121
16. Wang J, Tang W, Liang JC, Zhang L, Dai JY, Li X, Jin S, Cheng Q, Cui TJ (2024) Reconfigurable intelligent surface: power consumption modeling and practical measurement validation. IEEE Trans Commun. https://doi.org/10.1109/TCOMM.2024.3382332
17. Khan WU, Lagunas E, Mahmood A, Chatzinotas S, Ottersten B (2024) Ris-assisted energy-efficient leo satellite communications with noma. IEEE Trans Green Commun Netwo 8(2):780–790. https://doi.org/10.1109/TGCN.2023.3344102
18. Li H, Shen S, Nerini M, Clerckx B (2024) Reconfigurable intelligent surfaces 2.0: beyond diagonal phase shift matrices. IEEE Commun Magaz 62(3):102–108. https://doi.org/10.1109/MCOM.001.2300019
19. Nerini M, Shen S, Li H, Clerckx B (2024) Beyond diagonal reconfigurable intelligent surfaces utilizing graph theory: modeling, architecture design, and optimization. IEEE Trans Wireless Commun. https://doi.org/10.1109/TWC.2024.3367631
20. Mahmood A, Vu TX, Khan WU, Chatzinotas S, Ottersten B (2023) Joint computation and communication resource optimization for beyond diagonal uav-irs empowered mec networks. arXiv preprint arXiv:2311.07199

21. Li H, Shen S, Clerckx B (2023) Beyond diagonal reconfigurable intelligent surfaces: from transmitting and reflecting modes to single-, group-, and fully-connected architectures. IEEE Trans Wireless Commun 22(4):2311–2324. https://doi.org/10.1109/TWC.2022.3210706
22. Nerini M, Shen S, Clerckx B (2024) Closed-form global optimization of beyond diagonal reconfigurable intelligent surfaces. IEEE Trans Wireless Commun 23(2):1037–1051. https://doi.org/10.1109/TWC.2023.3285262
23. Li H, Shen S, Nerini M, Di Renzo M, Clerckx B (2024) Beyond diagonal reconfigurable intelligent surfaces with mutual coupling: modeling and optimization. IEEE Commun Lett 28(4):937–941. https://doi.org/10.1109/LCOMM.2024.3361648
24. Sun W, Sun S, Shi T, Su X, Liu R (2024) A new model of beyond diagonal reconfigurable intelligent surfaces (bd-ris) for the corresponding quantization and optimization. IEEE Trans Wireless Commun. https://doi.org/10.1109/TWC.2024.3382750
25. Mishra A, Mao Y, D'Andrea C, Buzzi S, Clerckx B (2024) Transmitter side beyond-diagonal reconfigurable intelligent surface for massive mimo networks. IEEE Wireless Commun Lett 13(2):352–356. https://doi.org/10.1109/LWC.2023.3329065
26. Guang Z, Liu Y, Wu Q, Wang W, Shi Q (2024) Power minimization for isac system using beyond diagonal reconfigurable intelligent surface. IEEE Trans Vehic Technol. https://doi.org/10.1109/TVT.2024.3385633
27. Li Q, El-Hajjar M, Hemadeh I, Shojaeifard A, Hanzo L (2024) Coordinated reconfigurable intelligent surfaces: non-diagonal group-connected design. IEEE Trans Vehic Technol. https://doi.org/10.1109/TVT.2024.3376985
28. Zhang C et al (2025) Sum rate maximization for 6g beyond diagonal ris-assisted multi-cell transportation systems. IEEE Trans Intell Transp Syst. https://doi.org/10.1109/TITS.2024.3521196
29. Ahmed M, Mirza MA, Raza S, Ahmad H, Xu F, Khan WU, Lin Q, Han Z (2023) Vehicular communication network enabled cav data offloading: a review. IEEE Trans Intell Transp Syst 24(8):7869–7897. https://doi.org/10.1109/TITS.2023.3263643
30. Wang H, Xiao P, Li X (2024) Channel parameter estimation of mmwave mimo system in urban traffic scene: a training channel-based method. IEEE Trans Intell Transp Syst 25(1):754–762. https://doi.org/10.1109/TITS.2022.3145363
31. Wang H, Memon FH, Wang X, Li X, Zhao N, Dev K (2023) Machine learning-enabled mimo-fbmc communication channel parameter estimation in iiot: a distributed cs approach. Digital Commun Netw 9(2):306–312
32. Ahmed M, Shahwar M, Khan F, Ullah Khan W, Ihsan A, Sadiq Khan U, Xu F, Chatzinotas S (2024) Noma-based backscatter communications: fundamentals, applications, and advancements. IEEE Internet Things J 11(11):19303–19327. https://doi.org/10.1109/JIOT.2024.3391219
33. Tseng P (2001) Convergence of a block coordinate descent method for nondifferentiable minimization. J Optim Theory Appl 109:475–494
34. Liu A, Lau V, Kananian B (2019) Stochastic successive convex approximation for non-convex constrained stochastic optimization. IEEE Trans Signal Process 67(16):4189–4203. https://doi.org/10.1109/TSP.2019.2925601
35. Grant M, Boyd S (2014) CVX: Matlab software for disciplined convex programming, version 2.1
36. Mahmood A, Vu TX, Khan WU, Chatzinotas S, Ottersten B (2022) Optimizing computational and communication resources for mec network empowered uav-ris communication. In: 2022 IEEE Globecom Workshops (GC Wkshps), pp. 974–979. IEEE
37. Chen Z, Ding Z, Dai X, Zhang R (2017) An optimization perspective of the superiority of noma compared to conventional oma. IEEE Trans Signal Process 65(19):5191–5202
38. Potra FA, Wright SJ (2000) Interior-point methods. J Comput Appl Math 124(1–2):281–302

Publisher's Note Springer Nature remains neutral with regard to jurisdictional claims in published maps and institutional affiliations.

Springer Nature or its licensor (e.g. a society or other partner) holds exclusive rights to this article under a publishing agreement with the author(s) or other rightsholder(s); author self-archiving of the accepted manuscript version of this article is solely governed by the terms of such publishing agreement and applicable law.

Authors and Affiliations

Manzoor Ahmed[1] · Wali Ullah Khan[2] · Mohammad Alamgeer[3] · Eatedal Alabdulkreem[4] · Shouki A. Ebad[5] · Ali M. Al-Sharafi[6] · Ashit Kumar Dutta[7] · Tahir Khurshaid[8]

✉ Manzoor Ahmed
manzoor.achakzai@gmail.com

Wali Ullah Khan
waliullah.khan@uni.lu

Mohammad Alamgeer
mabdoel@kku.edu.sa

Eatedal Alabdulkreem
eabdulkarem@pnu.edu.sa

Shouki A. Ebad
shoukeabaed@nbu.edu.sa

Ali M. Al-Sharafi
alsharafee@ub.edu.sa

Ashit Kumar Dutta
adotta@um.edu.sa

Tahir Khurshaid
tahir@ynu.ac.kr

[1] School of Computer and Information Science and Institute for AI Industrial Technology Research, Hubei Engineering University, Xiaogan City 432000, China

[2] Interdisciplinary Centre for Security, Reliability and Trust (SnT), University of Luxembourg, 1855 Luxembourg City, Luxembourg

[3] Department of Information Systems, College of Science & Art at Mahayil, King Khalid University, 62521 Abha, Saudi Arabia

[4] Department of Computer Sciences, College of Computer and Information Sciences, Princess Nourah Bint Abdulrahman University, 11671 Riyadh, Saudi Arabia

[5] Center for Scientific Research and Entrepreneurship, Northern Border University, 73213 Arar, Saudi Arabia

[6] Department of Computer Science and Artificial Intelligence, College of Computing and Information Technology, University of Bisha, 67714 Bisha, Saudi Arabia

[7] Department of Computer Science and Information Systems, College of Applied Sciences, AlMaarefa University, 13713 Diriyah, Saudi Arabia

[8] Department of Electrical Engineering, Yeungnam University, Gyeongsan 38541, Republic of Korea